The Journal of Neuroscience, October 15, 1998, *18*(20):8356–8368

Spine Loss and Other Persistent Alterations of Hippocampal Pyramidal Cell Dendrites in a Model of Early-Onset Epilepsy

Minghui Jiang, Chong L. Lee, Karen L. Smith, and John W. Swann

The Cain Foundation Laboratories, Department of Pediatrics and Division of Neuroscience, Baylor College of Medicine, Houston, Texas 77030

To explore the anatomical substrates for network hyperexcitability in adult rats that become chronically epileptic after recurrent seizures in infancy, the dendritic and axonal arbors of biocytin-filled hippocampal pyramidal cells were reconstructed. On postnatal day 10, tetanus toxin was unilaterally injected into the hippocampus and produced brief but recurrent seizures for 1 week. Later, hippocampal slices taken from these rats exhibited synchronized network bursts in area CA_{3C}. Both the apical and basilar dendritic arbors of CA_{3C} pyramidal cells were markedly abnormal in these epileptic rats. There was a considerable reduction in the density of dendrite spines, although the extent of this loss could vary among dendritic segments. Spine density on terminal segments of the basilar and apical dendrites was reduced on average by 35 and 20%, respectively. In addition, the diameters of these same dendritic segments were markedly reduced. Dendritic spine loss has previously been suggested to indicate a partial deafferentation of epileptic neurons, but this interpretation is difficult to reconcile with the critical role recurrent excitatory synaptic transmission plays in the generation of synchronized network burst. In this study, axonal arbors of CA_{3C} pyramidal cells exhibited normal branching patterns, branching complexity, and varicosity density. This suggests that if deafferentation occurs, synapses other than recurrent excitatory ones are lost. The morphological abnormalities reported here would be expected to significantly alter electrical signaling within dendrites that may contribute importantly to seizures and other behavioral sequelae of early-onset epilepsy.

Key words: hippocampus; dendrites; dendritic spines; axons; seizures; synapses

Dendrites of hippocampal pyramidal cells are morphologically complex and receive tens of thousands of excitatory synaptic contacts. Although historically, dendrites of central neurons were thought to play a passive role in synaptic integration (Johnston et al., 1996), more recent studies have shown the existence of voltage-dependent channels in the plasma membrane of pyramidal cell dendrites (Magee and Johnston 1995; Spruston et al., 1995; Hoffman et al., 1997). Results suggest channel distribution is far from homogeneous, and subsets of dendritic branches likely have different physiological properties. Thus, a complete understanding of the functional properties of hippocampal pyramidal cells will probably require detailed information of both the microanatomy and biophysical properties of individual dendritic segments.

Morphological alterations of dendritic arbors are likely to have important consequences on neuronal functioning. Indeed, dendrites appear to be anatomically plastic (Cross and Globus, 1978; Woolley et al., 1990; Mantyh et al., 1995; Collin et al., 1997). This adaptability is especially prominent during development (Leuba and Garey, 1984; Rhin and Claiborne, 1990; Dalva et al., 1994; Dailey and Smith, 1996) and is particularly evident in recent studies of dendritic spines (Moser et al., 1994; Hosokawa et al., 1995; Collin et al., 1997). Dendritic abnormalities have also been described in human diseases (Purpura et al., 1982; Catala et al., 1988; Ferrer et al., 1991), particularly in focal epilepsy. Studies have consistently reported reductions in dendritic spine density on pyramidal cells from epileptic patients. In addition, a loss of dendritic branches and varicose swellings are commonly observed on the remaining dendrites (Ward, 1969; Isokawa and Levesque, 1991; Multani et al., 1994; Belichenko and Dahlstrom, 1995; Isokawa et al., 1997). Studies of animal models of chronic focal epilepsy (Westrum et al., 1964; Reid et al., 1979; Willmore et al., 1980; Paul et al., 1981) have reported similar dendritic changes.

The majority of individuals with epilepsy have their first seizure in early childhood. It has been suggested that severe early-life seizures may alter the developing brain by damaging neurons (Falconer et al., 1964). However, in the few studies that have examined the long-term consequences of early-life seizures, the majority have been of models of single prolonged seizures (Nitecka et al., 1984; Okada et al., 1984; Cavalheiro et al., 1987). Results have suggested that immature neurons are relatively invulnerable to seizure-induced damage. Few studies have examined the consequences of recurrent seizures on the developing brain, although clinically this is a commonly observed feature of the childhood epilepsies.

Our laboratory has developed a model of early-onset epilepsy that is characterized by recurrent seizures in early life (Lee et al., 1995). Infant rats that receive a unilateral intrahippocampal injection of tetanus toxin experience brief, recurrent seizures for ~7 d. In adulthood, the majority of these animals are chronically epileptic (Lee et al., 1995). When hippocampal slices are taken from these adult rats, they produce spontaneous synchronized network discharges (Smith et al., 1998). In experiments reported here, individual neurons in slice preparations were intracellularly

Received April 6, 1998; revised July 20, 1998; accepted July 31, 1998.

This work was supported by National Institutes of Health Grants NS18309 and NS11535 from National Institute of Neurological Diseases and Stroke. We thank Dr. Martha Pierson for editing an earlier version of this paper and Dr. Kay Dunn for statistical advice.

Correspondence should be addressed to Dr. John W. Swann, The Cain Foundation Laboratories, Department of Pediatrics, Baylor College of Medicine, 6621 Fannin, MC 3-6365, Houston, TX 77030.

injected with biocytin. The morphological features of these cells were analyzed to uncover possible anatomical substrates for chronic network hyperexcitability.

Portions of this work have appeared in abstract form (Swann et al., 1996).

MATERIALS AND METHODS

Stereotaxic injection of tetanus toxin. Wistar rat pups (Harlan Sprague Dawley, Indianapolis, IN), 10 d of age, were anesthetized with an intraperitoneal injection of ketamine and xylazine (33 and 1.5 mg/kg, respectively). When necessary, this was supplemented by inhalation of methoxyflurane (Metofane). We dissolved 2.5 or 5 ng of tetanus toxin in 20 or 40 nl of sterile saline and injected it into the right hippocampus. The tetanus toxin used in this study was a gift of the Massachusetts State Biological Labs. The potency of the toxin was assayed by hindlimb paralysis after injection into the gastrocnemius muscle. The minimal dose (MD_{100}) that produced paralysis in all mice in a group ($n = 5$) was 0.25 ng (Lee et al., 1995). The surgical procedures and use of tetanus toxin were approved by an Animal Protocol Review Committee, the Infectious Agent and Hazardous Chemical Subcommittee, and the Animal Biosafety Subcommittee of Baylor College of Medicine. All procedures were in keeping with guidelines established by the National Institutes of Health.

To inject tetanus toxin, the pups were placed in an infant rat stereotaxic headholder, a midline incision was made, and a small hole was drilled in the skull. The stereotaxic coordinates for injection were: anteroposterior, −2.1 mm; mediolateral, 3.0 mm from the bregma; and dorsoventral, −2.95 mm from the dural surface. The toxin was slowly injected at 4 nl/min. After injection, the needle was left in place for 15 min to reduce reflux up the needle track. During injections, the body temperature of rat pups was maintained by a warmed (electrically regulated) metal plate. Littermates, stereotaxically injected with sterile saline, or untreated rats served as controls.

Behavioral monitoring of seizures in infant rats. The frequency of behavioral seizures was monitored for 1 hr/day for 10 consecutive days after tetanus toxin injections. The types and duration of seizures were scored. Wild running seizures were most easily identified. Rats that had a total of two or more wild running seizures during the 10 monitoring sessions were selected for *in vitro* slice studies when they reached adulthood. Besides seizure, no other behavioral signs of neurological abnormalities were observed in tetanus toxin-treated rats.

In vitro *slice procedures.* Hippocampal slices were prepared from adult rats (experimentals = 19, controls = 26) that were 35–60 d of age. Slices were prepared by methods previously described (Smith et al., 1995, 1998). After anesthesia with metofane, the forebrain was removed and the right and left hemispheres separated. Slices (500-μm-thick) were prepared from both the injected and contralateral hippocampus and were usually obtained from the dorsal hippocampus. Routinely, slices from littermate control rats were placed in the chamber beside those from experimental animals to facilitate comparisons under identical experimental conditions. The chamber was constantly perfused with an artificial CSF (ACSF) containing (in mM): 123 NaCl, 3.5 KCl, 1.5 $CaCl_2$, 1.5 $MgSO_4$, 1.25 $NaHPO_4$, 26 $NaHCO_3$, and 10 glucose. The perfusate was bubbled with 95% O_2 and 5% CO_2. Temperature was maintained at 32–33°C.

After a 1 hr recovery period, electrophysiological recordings were begun using standard techniques. Intracellular and extracellular field recordings were obtained using glass microelectrodes. Extracellular electrodes were filled with NaCl (2 M) and had resistances of 5–10 MΩ. All recordings were referred to a remote silver–silver chloride bath ground. Slices were first surveyed for the presence of abnormal epileptiform activity by recording field potentials at various locations in the pyramidal cell body layer. At each location, recordings were made for 5–10 min. When abnormal activity was observed, discharges were recorded in a number of nearby sites in the cell body layer to locate the site at which discharges were the most robust.

Intracellular recordings were made at sites in which spontaneous epileptiform discharges were the largest. This was always in hippocampal area CA_{3C} (Smith et al., 1998). These recordings were made with glass microelectrodes, whose tips contained 3–5% biocytin dissolved in 0.5 M KCl. These electrodes were backfilled with 0.5 M KCl and had resistances of 80–150 MΩ. In both experimental and control rats, filled neurons had resting membrane potentials greater than −50 mV and overshooting action potentials. To avoid neurons whose dendrites were cut during slicing, recordings were always made at least 100 μm from the upper surface of the slice. Biocytin was iontophoresed intracellularly by passing hyperpolarizing current.

All electrophysiological recordings were stored on tape for later analysis. Selected signals were collected with software developed for a personal computer. Signals were digitized at 10 kHz. Hard copies were obtained from a laser jet printer.

Biocytin histochemistry. Slices were fixed overnight in 4% paraformaldehyde in 0.1 M PBS, pH 7.4, and 5% sucrose. The tissue was rinsed and stored in PBS. Thereafter, slices were embedded in 4% agar and resectioned (50 μm) on a vibratome. Biocytin was visualized by avidin-D horseradish peroxidase (Vector Laboratories, Burlingame, CA) histochemistry (Gomez-DiCesare et al., 1997). A free-floating method for tissue processing was used. After the horseradish peroxidase reaction, sections were mounted on gelatinized slides, dried, dehydrated, and coverslipped with DPX. Selected labeled cells were photographed using a Nikon Microphot FXA microscope.

Neuron reconstruction. CA_3 pyramidal cells were labeled in 89 slices from control and 62 slices from experimental rats. To be accepted for analysis, a cell had to meet the following criteria: (Gomez-DiCesare et al., 1997) (1) only a single pyramidal cell was labeled, (2) the biocytin label did not fade in the course of a process, (3) processes were darkly stained with clearly visible details such as spines and varicosities, (4) label reached either natural-appearing terminations or artificially cut endings at the surfaces of the section, (5) the plane of the slice was parallel to the predominant plane of the dendritic arbors, and (6) the cell and its arbors appeared to be centered within the depth of the slice.

Of the 62 slices from tetanus toxin-treated rats, 22 contained a single neuron that met all of our criteria. In slices from control rats, 38 neurons in 89 slices met the criteria for acceptance. The dendritic and axonal arbors of selected cells (see Results) were reconstructed in their entirety through each section of the slice with the Eutectic neuron reconstruction system (Sun Technologies, Durham, NC). All reconstructions were made using a 100× oil immersion objective (Olympus-BH-2 microscope). The investigator performing the reconstructions was blinded to the group (experimental vs control) from which each sample was taken. Parameters analyzed included the locations of branch points on the dendrites and axons and the locations of varicosities on the axonal arbors. Varicosities were counted only if they were >1.5 times the diameter of the adjacent axon. Dendritic spines were counted if they were well stained with clearly demarcated boundaries against the background and adjacent structures. Detailed spine counts were performed on all terminal branches of randomly selected second order apical and first order basilar dendrites. On average, spine counts were obtained from 14 terminal order dendrites in each cell. The length of each terminal branch was determined by finding a naturally occurring end of a dendrite and following this segment backward toward the soma until the first branch point was encountered. The minimal and maximal diameters of terminal order dendrites was also measured (using a 100× objective). This was accomplished by varying the size of the cursor used in the Eutectic system to trace the dendritic segments. The minimal and maximal diameters for each segment were the smallest and largest diameters measured by this cursor.

Thorny excrescences were considered as individual structures when they were separated from nearby excrescences by an easily identified dendritic shaft. The area of these excrescences was measured in two dimensions in the focal plane that gave the largest cross-sectional area. These measures were achieved by reconstructing the outline of individual excrescences with the Eutectic system. The extent of individual axon arbors was also examined by using a Sholl analysis (Sholl, 1955) in which Eutectic software generated a series of concentric 25 μm circles that were centered on the soma of a neuron. Axon crossings of each of these circles were considered a measure of axon arbor complexity at increasing distances from the parent neuron.

To depict alterations in dendritic spine density, the dendrites of selected CA_3 pyramidal cells were also drawn using camera lucida techniques. A 100× oil immersion objective was used.

Statistics. The *t* test for comparison of two independent means was used in comparing features of dendritic and axon arbors in experimental and control rats. Because multiple *t* tests were performed on data in Table 1, significant values of $p < 0.05$ should be cautiously interpreted. When data were not normally distributed, a Mann–Whitney *U* test was used. Results from Sholl analyses were analyzed by a repeated measures two-way ANOVA. Sigma Stat was used to perform all statistical tests.

Table 1. Comparison of the morphological features of CA_{3C} hippocampal pyramidal cell dendrites and axons in control and experimental rats

	Apical		Basilar		Total	
Parameters	Control	Experimental	Control	Experimental	Control	Experimental
n	6	6	6	6	6	6
Dendrites						
Spine density (number/100 μm)[a]	46.2 ± 2.5	36.5 ± 5.3**	49.5 ± 4.7	31.6 ± 6.4***	47.8 ± 2.8	34.0 ± 4.9***
Diameter[a]						
Minimal (μm)	0.40 ± 0.08	0.18 ± 0.04***	0.37 ± 0.07	0.24 ± 0.04**	0.39 ± 0.07	0.22 ± 0.04***
Maximal (μm)	0.50 ± 0.14	0.26 ± 0.06**	0.43 ± 0.08	0.29 ± 0.07**	0.47 ± 0.11	0.28 ± 0.06**
Thorny excrescences						
Number	6.50 ± 1.39	2.83 ± 1.72**	6.00 ± 4.14	3.83 ± 3.13	12.5 ± 4.41	6.67 ± 4.32*
Area (μm^2)	55.9 ± 31.1	73.7 ± 71.8	39.0 ± 21.3	45.8 ± 39.2	50.6 ± 12.1	66.4 ± 29.8
Segment number	75.5 ± 26.1	67.8 ± 25.8	73.3 ± 16.0	51.2 ± 13.4*	143 ± 35.8	124 ± 9.4
Length (mm)	4.64 ± 1.42	4.43 ± 0.76	3.96 ± 0.77	3.01 ± 0.98	8.60 ± 1.63	7.45 ± 0.73
Axons						
Length (mm)	4.02 ± 1.6	4.81 ± 3.0	5.20 ± 1.83	5.26 ± 2.21	9.23 ± 2.95	10.1 ± 4.49
Branch number	28.0 ± 15.5	27.5 ± 19.3	59.8 ± 19.1	53.2 ± 25.1	87.8 ± 28.4	80.7 ± 37.4
Varicosity number	396 ± 215	481 ± 302	771 ± 422	629 ± 293	1167 ± 571	1111 ± 437
Varicosity density (number/100 μm)	9.38 ± 3.70	9.97 ± 3.70	14.27 ± 3.83	11.75 ± 2.27	12.02 ± 3.45	10.86 ± 1.10

[a]Measures are from terminal order dendritic segments, $n = 6$. Six neurons were reconstructed in both the experimental and control groups. Data are expressed as mean ± SD.
*$p < 0.05$.
**$p < 0.01$.
***$p < 0.001$.

RESULTS

Seizures in infant rats

One to two days after unilateral injection of tetanus toxin into the right dorsal hippocampus, 100% ($n = 34$) of 10-d-old rat pups developed a severe epileptic syndrome. Typically, rats underwent recurrent behavioral seizures that consisted of wild running episodes, prolonged wet dog shakes, and forelimb clonus. These behaviors often occurred in constellations, but could occur separately. During a total of ten daily 1 hr monitoring sessions, an average of 6.1 ± 3.0 wild running seizures were observed. These seizures were usually 30 sec to 2 min in duration. More prolonged seizures (>3 min) were rarely observed. Previous EEG recordings have demonstrated that electrographic seizures occur concurrently with these behaviors (Lee et al., 1995; Anderson et al., 1997). These discharges arise not only from the injected hippocampus but from contralateral hippocampus and bilaterally within neocortex. Rats that displayed more than two behavioral seizures during the ten 1 hr monitoring sessions were chosen for *in vitro* slice studies. Of the 34 rats injected with tetanus toxin, 19 were used in *in vitro* experiments reported here. On occasion, rats were observed in adulthood to have unprovoked behavioral seizures. However, these events were usually infrequent, and adult rats were not monitored for behavioral seizures before *in vitro* slice recordings were undertaken.

Epileptiform activity recorded in *in vitro* slices from adult rats

Spontaneous epileptiform activity was recorded in slices from 16 of 19 (84%) experimental rats but was never observed in slices from 26 control rats [$\chi^2 = 30.4$, degrees of freedom = 1, $p < 0.001$ when comparing experimentals (16 of 19 rats) to controls (0 of 26)]. As reported previously (Smith et al., 1998), epileptiform discharges were recorded in both the tetanus toxin-injected and the contralateral hippocampus. These results are fully consistent with EEG recordings that demonstrate interictal spikes in either hippocampus in chronically epileptic rats (Anderson et al., 1998). Of slices displaying epileptiform activity, 50% (11/22) were from the injected and 50% from the contralateral hippocampus. Epileptiform discharges were largest in area CA_{3C} in which stratum pyramidale courses between the upper and lower blades of the granule cell body layers of the dentate gyrus. Figure 1 is an example of these events. Intracellularly (traces 1), individual neurons underwent an intense depolarization shift that was usually 10–30 mV in amplitude and 50–100 msec in duration. The intracellular depolarizations resulted in a burst of action potentials and occurred simultaneously with extracellularly recorded network burst discharges (traces 2) that reflected the synchronous discharging of CA_3 pyramidal cells. When slices from a rat displayed epileptiform activity, neurons were injected intracellularly with biocytin. When slices from experimental rats did not display epileptiform activity, further studies of this tissue were not undertaken. In slices from control rats, neurons in the pyramidal cell body layer of area CA_{3C} were verified to have the intrinsic physiological properties of CA_{3C} pyramidal cells before being injected with biocytin.

Morphological features of pyramidal cells in area CA_{3C}

Individual CA_{3C} pyramidal cells from experimental and control rats were subjected to detailed morphological comparisons to explore possible anatomical substrates for hippocampal hyperexcitability in adulthood. In area CA_{3C}, pyramidal cells have a variety of dendritic morphologies. A subclass of neurons was selected for study. These were called "windblown" pyramidal cells because their apical dendrites appear to bend in an attempt to avoid the suprapyramidal blade of the granule cell body layer in the dentate gyrus (Buckmaster et al., 1993). We restricted morphological analysis to this single neuronal subtype to avoid differences in the microanatomy between subclasses of pyramidal cells. We reasoned that an introduction of cell to cell variations (caused by inclusion of a variety of neuronal subclasses in our

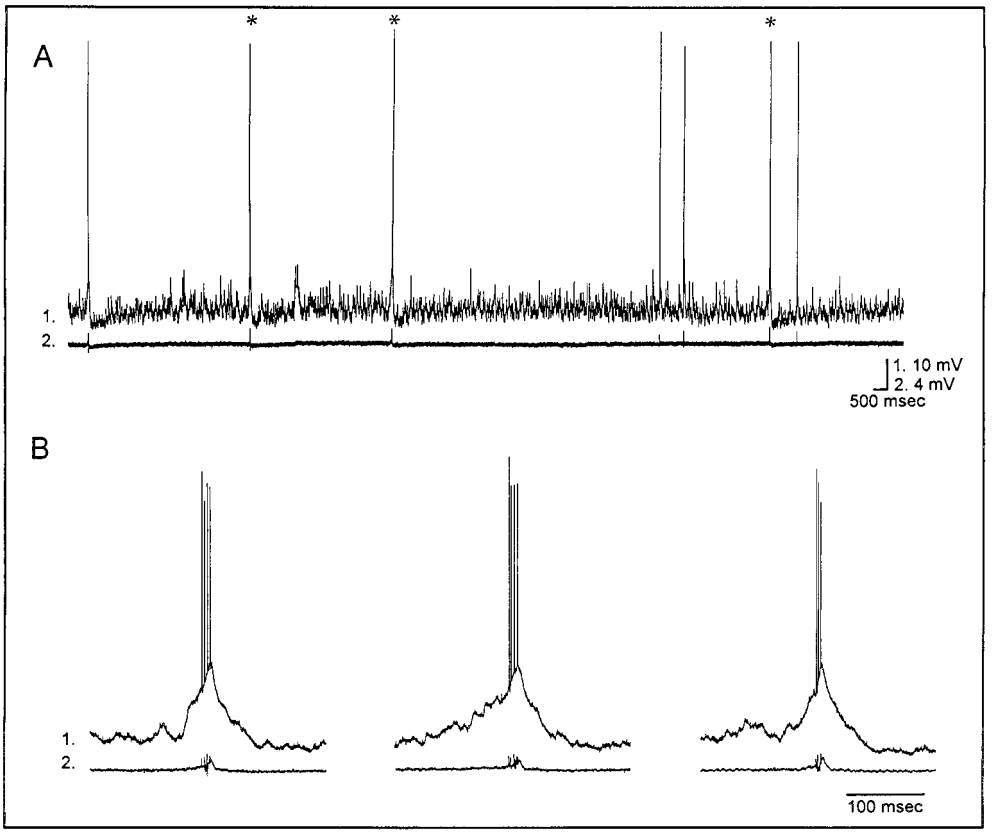

Figure 1. Synchronized network bursting recorded in an adult rat hippocampal slice after tetanus toxin injection in infancy. *A*, Simultaneous intracellular (*1*) and extracellular (*2*) field recordings illustrate the frequency of events that occurred spontaneously in normal ACSF. Selected events (*) in *A* are shown in *B* at a faster time base. This slice was obtained from a 57-d-old rat ipsilateral to tetanus toxin injection. Resting potential and input resistance: −59 mV, 70 MΩ.

database) would likely confound detection of abnormalities in epileptic compared with littermate control rats. A total of seven pyramidal cells with windblown dendrites were filled in slices from experimental rats and nine in controls. We selected six from each for detailed reconstructions and quantitative analysis. The remainder were used for qualitative comparisons. Of cells selected from experimental rats, two were from the hippocampus contralateral to tetanus toxin, and four were from the injected hippocampus.

Figure 2 demonstrates the basic anatomical features of this subtype of CA_{3C} pyramidal cell. Typical for hippocampal pyramidal cells, apical and basilar dendrites project into stratum radiatum and stratum oriens, respectively. However, these processes usually did not enter the hilus of the dentate gyrus. Indeed, in Figure 2*A*, two apical dendrites emerge from the cell body. The branch to the right projects locally in the CA_{3C} subfield but does not enter the hilus (H); instead it terminates some distance (~100 μm) from the upper blade of the granule cell body layer (GL). On the other hand, the primary apical dendrite on the left is much longer. It appears to avoid the granule cell body layer and projects into stratum lacunosum-moleculare of area CA_3. A higher magnification photomicrograph (Fig. 2*B*) of the dendrites near the cell body layer shows that both the proximal apical and basilar dendrites have large specialized dendritic spines or thorny excrescences (*arrows*) on their surface. As shown in Figure 2*C*, more distal apical (*right*) and basilar (*left*) dendrites are densely covered with spines. These spines are quite uniform in their distribution and extend to the most distal aspects of the terminal dendritic branches. The axon of this pyramidal cell emerges from the basal pole of the soma and projects to the left before branching (Fig. 2*A*, *arrowhead*) to form secondary axon collaterals, one of which can be seen projecting across stratum pyramidale. This collateral branches again as it projects toward the CA_{3B} subfield. A plexus of recurrent axon collaterals was present in the CA_{3C} subfield. Examples of these axons are shown at higher magnification in Figure 2*D*. These are studded with numerous varicosities (*arrows*), which are probable sites of synaptic contact with neighboring CA_3 pyramidal cells or local circuit interneurons. The majority of axons recovered in slice experiments remained in the same subfield of the parent neuron and interweave among its dendritic processes. The densest arbors were usually found in stratum oriens.

Dendritic abnormalities in chronically epileptic rats

When the morphological features of CA_{3C} pyramidal cells were compared in rats that had tetanus toxin-induced seizures and their controls, abnormalities were at first not obvious. Figure 3 compares computer reconstructions of the dendritic arbors from two experimental (*B*,*D*) and two control (*A*,*C*) rats. Slices were taken between postnatal days 40 and 48. The windblown features of the apical dendrites are immediately evident in all cells. Indeed, at least qualitatively, the dendritic branching pattern appears comparable in rats that had seizures in infancy and their controls. However, numerous abnormalities were observed at higher magnification in neurons from experimental rats. Among differences, there were dramatic localized reductions in the number of dendritic spines. The extent of spine loss could vary among processes in the same cell. In some instances, dendritic segments were nearly devoid of spines, but in others they appeared to have a normal spine density. Most often dendritic segments were between these two extremes and demonstrated localized reductions in spine density. Figure 4 shows four high-power photomicrographs of terminal order dendritic segments. Figure 4*A* shows a dendritic segment from a control rat in which dendritic spine

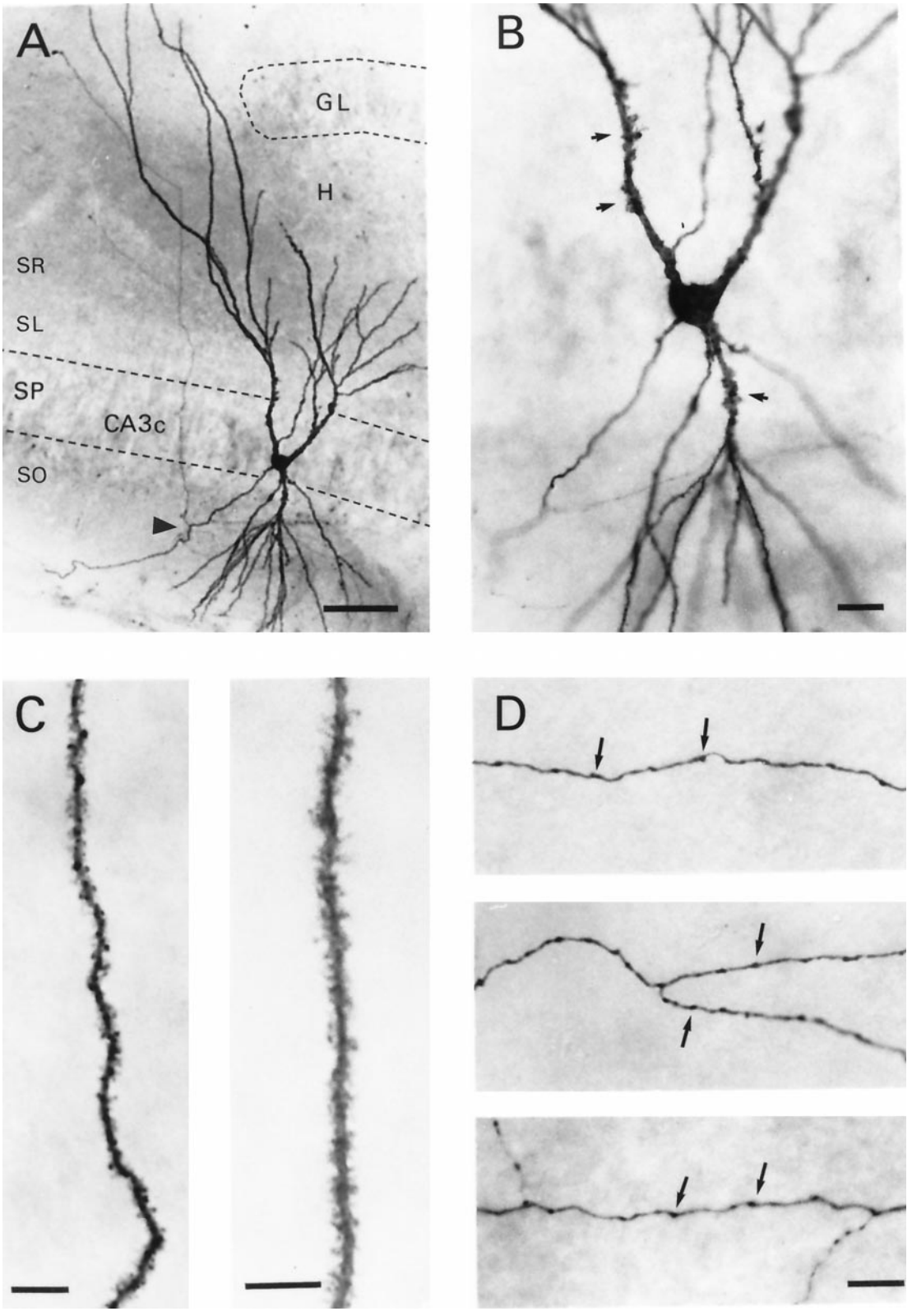

Figure 2. Morphological features of a CA_{3C} hippocampal pyramidal cell filled with biocytin. *A*, Photomicrograph shows a cell body located in stratum pyramidale (*SP*) and apical and basilar dendrites that project into stratum radiatum (*SR*) and stratum oriens (*SO*), respectively. Notice the lengthy apical dendrites that appear to bend to avoid the upper blade of the granule cell body layer (*GL*) of the dentate gyrus. This dendrite gives the cell a windblown appearance. The axon emerges from the basal pole of the soma and courses through stratum oriens before branching (*arrowhead*), sending a collateral to stratum radiatum. *B*, Higher magnification photomicrograph of the soma and proximal dendrites. *Arrows* denote selected thorny excrescences. *C*, An apical (*right*) and basilar (*left*) dendritic segment shown at higher magnification. Note the uniform density of dendritic spines that covers these processes. *D*, Portions of the axon arbor emanating from this cell. *Arrows* denote varicosities on these axon branches. *H*, Hilus of dentate gyrus; *SL*, stratum lucidum. Scale bars: *A*, 50 μm; *B*, 20 μm; *C*, 10 μm; *D*, 10 μm.

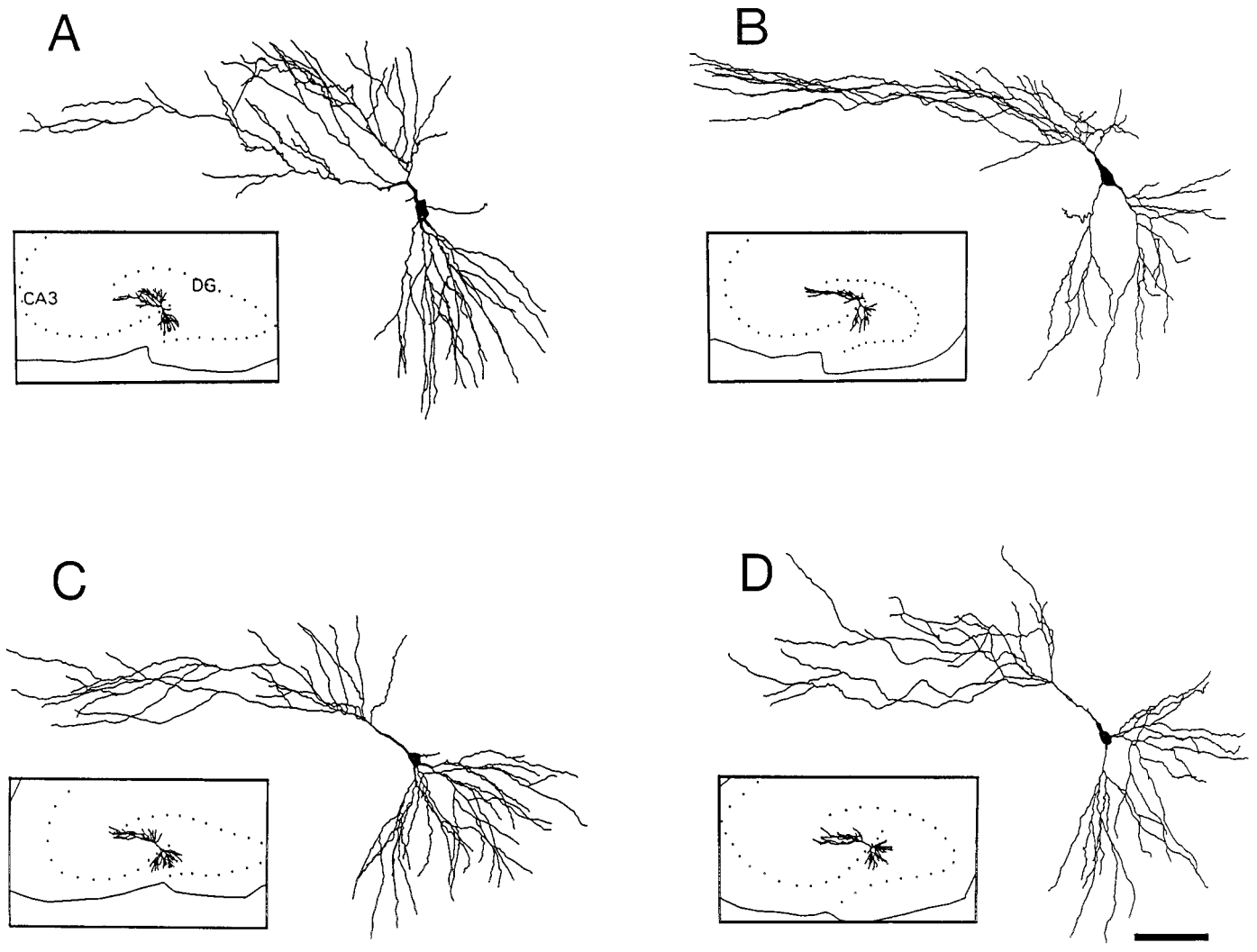

Figure 3. Comparison of dendritic arbors in two control (*A*, *C*) and two chronically epileptic (*B*, *D*) rats. The somas and dendrites were computer-reconstructed. The location of these neurons in the CA_{3C} subfield are shown in the *insets*. Notice the dramatic windblown appearance of the apical dendrites. *DG*, Dentate gyrus. Scale bar, 100 μm.

density is high and comparable to that in Figure 2*C*. In Figure 4*B*, spine loss is quite dramatic, and dendritic spines are rarely observed on this dendritic segment. In Figure 4, *C* and *D*, spine loss is also marked, although less dramatic than in Figure 4*B*. Spines are apparent in some areas of these terminal order segments. Figure 4*D* also displays a second commonly observed abnormality of dendrites in the experimental group. Often, dendritic segments were reduced in diameter. This was particularly evident in the terminal order branches of both apical and basilar dendrites. The varicose swellings of dendritic segments typical of acute models of epilepsy and in tissue obtained after surgery in humans with uncontrolled temporal lobe epilepsy were not observed.

In Figure 5, camera lucida drawings are shown to illustrate spine loss and alterations in dendritic diameter of neurons from experimental rats. In Figure 5*A*, apical (*top drawings*) and basilar (*bottom drawings*) dendritic trees arising from single primary dendrites near the cell body are shown for a control (*left*) and an experimental rat (*right*). In the dendrites from the control rat, spines appear to be uniformly distributed on the dendritic surface, and their density is quite high. However, in the neuron from the experimental animal (Fig. 5*A*, *right*), dendritic spine density is dramatically reduced in both the apical and basilar dendritic trees. In this cell, all segments showed a reduction in the number of spines. Figure 5, *B* and *C*, gives a more detailed view of selected portions (Fig. 5*A*, *arrows*) of the apical and basilar dendrites, respectively. As is evident in Figure 5*A*, spine loss is quite marked. Spine density was, on average, 37 spines/100 μm on the apical dendrites in Figure 5*A* (from the control rat). Spine density was 19 spines/100 μm on the apical dendrites from the experimental rat. Reconstructions of the basilar dendrites gave similar results. There were 37 spines/100 μm in the dendrites from the control rat and only 16 spines/100 μm in the cell from the experimental rat. A reduction in the diameter of the dendritic shafts is also evident in Figure 5. In this neuron, the minimal and maximal diameter of six terminal segments selected from the apical dendrites were on average 0.12 ± 0.04 μm and 0.16 ± 0.05 μm, respectively, whereas diameters of six comparable dendrites from the control rats had values between 0.42 ± 0.04 μm and 0.48 ± 0.04 μm. Similar differences were observed in dendritic diameters in the basilar dendrites of these cells. Spine loss and the reduction in dendritic diameter were similar for neurons taken ipsilateral and contralateral to tetanus toxin injection.

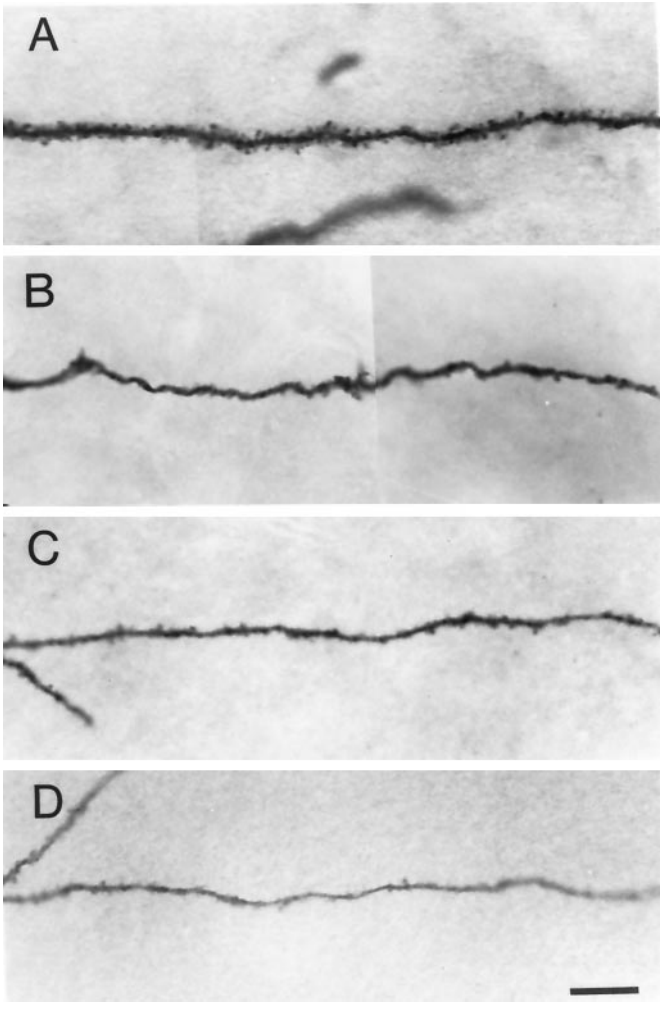

Figure 4. Comparison of spine density on dendritic segments of CA_{3C} hippocampal pyramidal cells from a control and three experimental rats. *A* shows a dendritic segment from a control rat. Note the density of spines. *B–D* are examples of dendritic segments of three pyramidal cells from three separate epileptic rats. In *B*, spine density is severely reduced. In *C* and *D*, spines are present but greatly reduced in number. Often the diameters of dendritic shafts are reduced in experimental rats. This is evident in *D*. Scale bar, 10 μm.

The results of analysis of all the neurons that were reconstructed are summarized in Figure 6 and Table 1. Figure 6 is composed of scatter diagrams that compare spine density (*A*) and maximal dendritic diameter (*B*) in the biocytin-filled CA_{3C} pyramidal cells. Each dot is the average value from terminal order segments in apical and basilar dendrites. Results show that in the population as a whole, there was a significant decrease in spine density and dendritic diameter. In the basilar dendrites there was, on average, a 35% decrease in spine density. A 20% decrease was observed in the apical dendrites. When both dendritic arbors were analyzed together, nearly a 30% decrease was observed. These data are summarized in Table 1. Differences in measurements of both the minimal and maximal diameter of the dendritic segments were equally dramatic. For instance, the minimal diameter of the terminal segments of the apical and basilar dendrites was reduced, on average, by 55 and 35%, respectively. Similar reductions in maximal diameters (48 and 33%) were also found (Table 1). When data from both dendritic arbors were combined, a 44 and 40% decrease in the minimal and maximal diameters of dendritic segments was observed.

Other morphological changes were observed. Thorny excrescences are highly specialized dendritic spines on CA_3 neurons that receive giant mossy fiber synaptic terminals (Claiborne et al., 1986; Chicurel and Harris 1992). These presynaptic terminals are located on mossy fiber axons that emanate from the dentate granule cells. In keeping with the observed decrease in spine density in pyramidal cells in experimental rats (Figs. 4–6), analysis of thorny excrescences on CA_{3C} pyramidal cells showed a 47% decrease in the number of excrescences. Apical dendrites showed the most dramatic and consistent effect with a 57% decrease in the number of thorny excrescences (Table 1). Photomicrographs in Figure 7 compare thorny excrescences on the proximal apical dendrites of pyramidal cells from a control (*A*) and an experimental (*B*) rat. In the neuron from the control rat, numerous thorny excrescences can be seen, some of which are denoted by arrows. Thorny excrescences were always present and in high number on CA_{3C} pyramidal cells from control rats. However, in the cell from the experimental rat (Fig. 7*B*), the number of thorny excrescences were dramatically reduced. Indeed, in this cell (as well as in one other obtained from experimental rats, but not reconstructed) thorny excrescences were completely absent. Nonetheless, the majority of pyramidal cells from experimental rats possessed thorny excrescences, although in reduced numbers. The excrescences that remained were equal in size (as measured by area) to those in control rats (Table 1).

Total length of the apical and basilar dendrites was smaller, but not significantly so, in experimental rats. For instance, the basilar dendrites were 24% shorter in experimental animals. On the other hand, the number of basilar dendritic segments was significantly reduced (30%; Table 1) in experimental rats. This suggests a loss of dendritic mass may accompany the changes in dendritic spine and dendritic diameter in this experimental model of epilepsy.

Recurrent excitatory axonal arbors in chronically epileptic rats

Marked dendritic spine loss, as seen in the experimental animals of this study, has long been thought to be a sign of dendritic deafferentation (Hámori, 1973; Parnavelas et al., 1974; Matthews et al., 1976; Represa et al., 1991). A major excitatory synaptic input onto both the apical and basilar dendrites of CA_3 pyramidal cells is supplied by recurrent excitatory synapses that arise from nearby pyramidal cells. We reasoned that if pyramidal cell dendrites were deafferented, then the extent and complexity of local circuit axon arbors emanating from CA_3 neurons should also be reduced. To address this issue, the axon arbors from the 12 biocytin-filled neurons from the experimental and control animals were reconstructed.

Representative axon arbors are shown in Figure 8. As shown in Figure 8*A–D*, the patterns of local axonal projections in neurons from experimental (*C*,*D*) and control rats (*A*,*B*) were similar. In both groups, axon arbors ramified extensively in the CA_{3C} subfield. The most complex arbors were found in stratum oriens near the soma and basilar dendrites of the parent neuron. In all neurons, individual axon collaterals projected through stratum oriens of the CA_{3C} subfield and entered the hilus of the dentate gyrus. There, they would branch locally, apparently to innervate neuronal elements in the hilus. In some instances, these axons were quite long. They not only reached the granule cell layer, but projected for short distances into the molecular layer of the

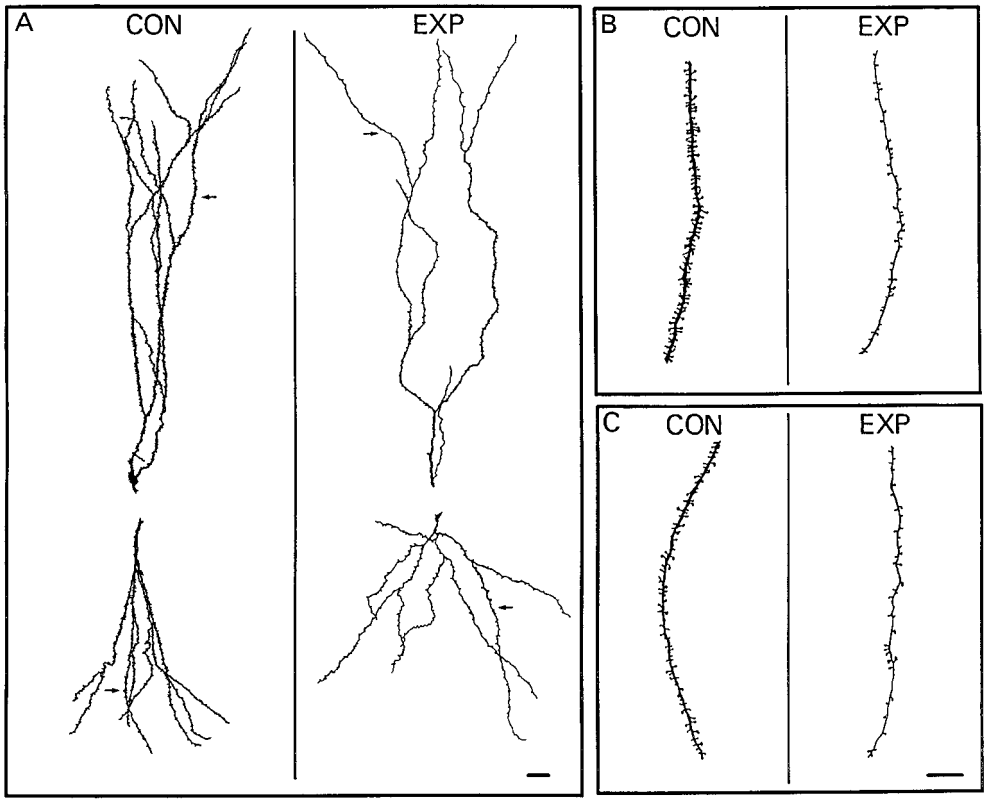

Figure 5. Camera lucida drawings comparing the apical and basilar dendrites from a control and an experimental rat. *A*, Apical (*top drawing*) and basilar (*bottom drawing*) dendritic trees arising from a single proximal dendrite near the cell body are shown. Spine density is reduced throughout the arbors in the dendrites from the experimental rat. *Arrows* in *A* denote apical and basilar segments that are enlarged in *B* (apical) and *C* (basilar). Drawings on the *left* in each panel are from a neuron in a control (*CON*) animal, whereas those on the *right* are from an experimental (*EXP*) rat. Scale bars: *A*, 20 μm; *B*, *C*, 10 μm.

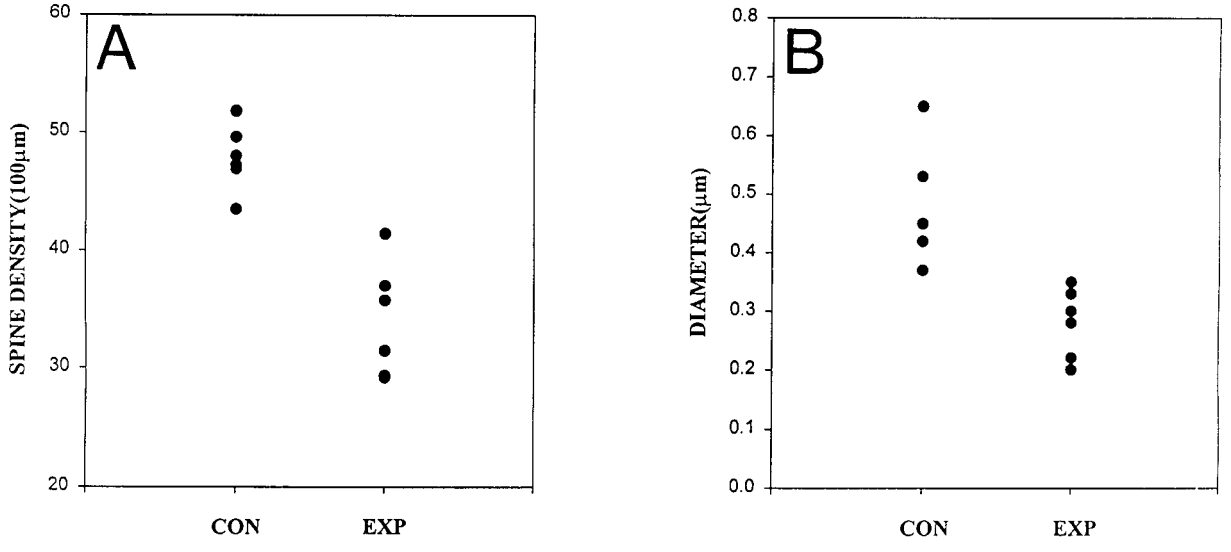

Figure 6. Scatter diagrams compare dendritic spine density and maximal dendritic diameter in control and experimental rats. Data were derived from an analysis of terminal dendritic segments of six neurons in control (*CON*) and experimental (*EXP*) rats. The average spine density and maximal dendritic diameter for each neuron are plotted. *A* Spine density is reduced. *B*, Maximal dendritic diameter is reduced in neurons from experimental rats.

dentate. Additionally, all neurons had at least one, and often several, axon collaterals that crossed the CA_{3C} cell body layer. Once in stratum radiatum, the axons had several apparent targets. First, they ramified locally in stratum radiatum near the parent neurons. Second, one or more axons would continue into the CA_{3A} and CA_{3B} subfield in which the axons would usually terminate as a cut end (*asterisks*) on the slice surface. These axons likely contribute to the Schaffer collaterals system in CA_1. Indeed, in two slices (one from an experimental rat and one from a control) these axons were not cut and projected as a single axon into stratum radiatum of area CA_1 (Fig. 8*D*). In a third pattern of axonal projection, axons instead of projecting toward area CA_{3A} and CA_{3B} turned into the hilus in which they ramified. On occasion, these fibers reached the upper blade of the granule cell body layer.

Although the patterns of local axonal projections were similar in the experimental and control groups, we undertook a Sholl analysis (Sholl, 1955) of axonal arbors to determine whether there

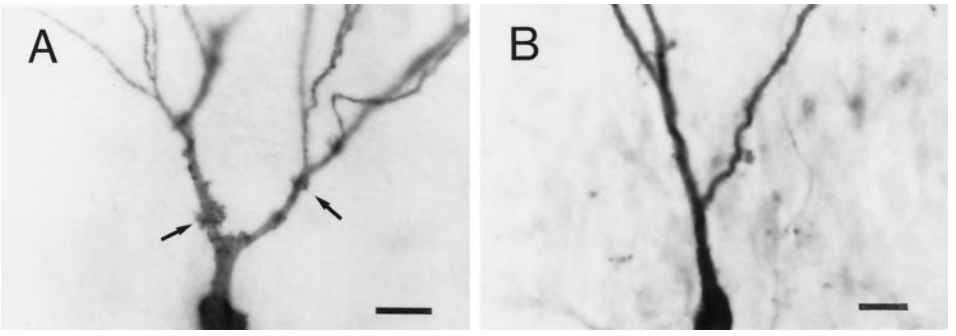

Figure 7. Photomicrographs comparing the density of thorny excrescences on apical dendrites of pyramidal cells from a control and an experimental rat. *A* shows the proximal apical dendrites of a neuron from a control rat. Selected thorny excrescences are denoted by the *arrows*. *B* shows the proximal apical dendrites of a pyramidal cell from an experimental rat. Dendrites are devoid of thorny excrescences. Scale bars: *A*, 20 μm; *B*, 20 μm.

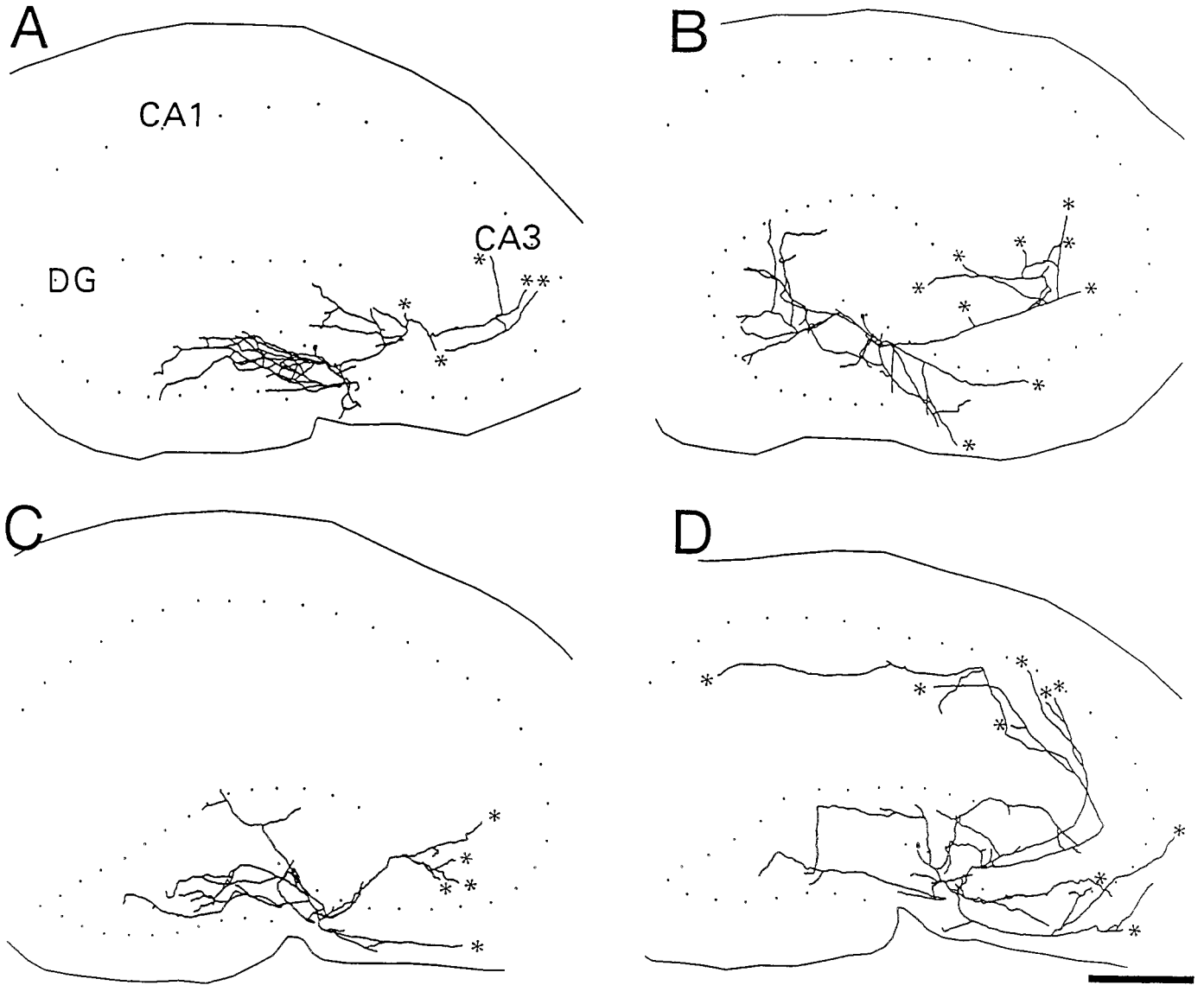

Figure 8. Comparison of recurrent axon arbors emanating from CA_{3C} pyramidal cells in control and experimental rats. *A* and *B* show computer-reconstructed axon arbors from two control rats. *C* and *D* are from two experimental rats. *Dotted lines* depict the pyramidal and granule cell layers. The *solid lines* outline the natural surface of the slices. *Asterisks* denote artificial cut ends of Schaffer collaterals on the surface of slices. The general pattern of axonal arborization appears similar in samples from control and experimental rats. Scale bar, 500 μm.

were any changes in the extent of arborization in experimental animals. In this analysis, the cell body of each neuron was located in the center of concentric circles that were spaced at 25 μm intervals. To analyze the axon arbors, the number of axons that intersected each of these circles were counted. With a decrease in axon arborization (consistent with a deafferentation of CA_{3C}), pyramidal neurons would be expected to produce fewer circle intersections. Results are shown in Figure 9*A*. Other than a

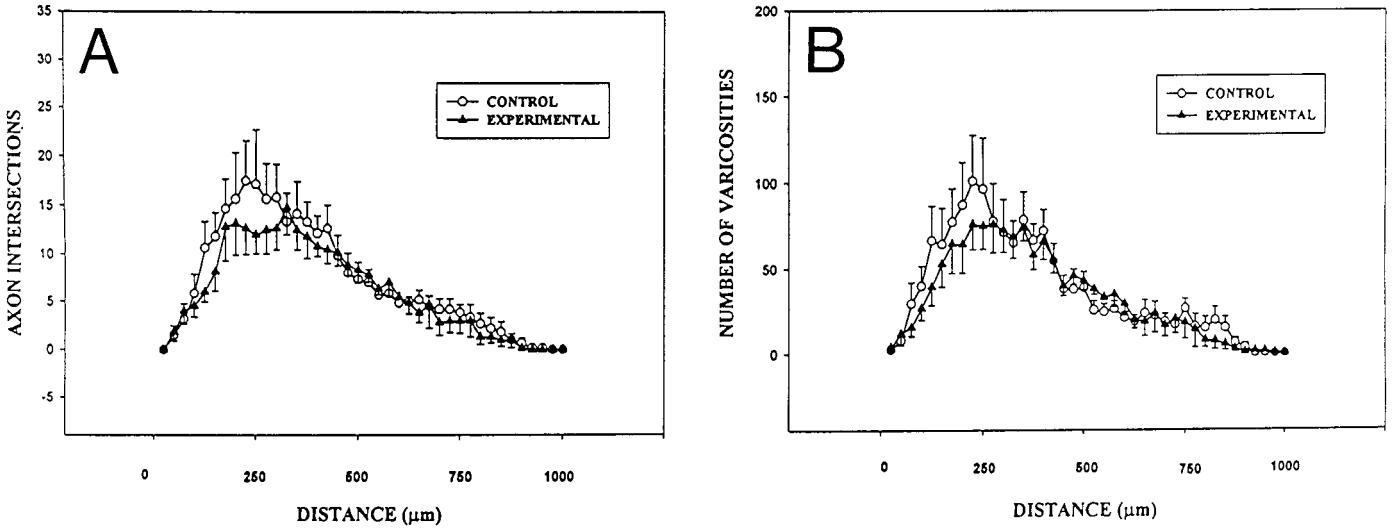

Figure 9. Sholl analysis of axon arbors and numbers of varicosities in control and experimental rats. *A*, Graph compares the mean number of axon intersections of concentric rings that were centered on the soma and spaced at 25 μm intervals. There appears to be a tendency for slightly fewer axon crossings 200–300 μm from the soma in neurons from experimental rats. *B*, Graph of the mean number of varicosities located within the concentric rings. Like results from axon intersections, slightly fewer varicosities were seen in experimental rats within 250 μm of the soma. Data expressed as $\bar{x} \pm$ SEM. A repeated measures two-way ANOVA was used to compare axon arbors from experimental and control rats. Measures of axons and varicosities from experimental rats were found not to be statistically different from those of the control group ($p > 0.05$).

tendency for axon arbors to be less complex close to (within 200–300 μm) the soma of the parent neuron, the overall pattern of axon arborization was very similar in the experimental and control groups. The number of intersections was largest at 250 μm from the soma and gradually decreased with increasing distance. An analysis (a repeated measures two-way ANOVA) of the results in Figure 9*A* showed that the difference between axons in control and experimental rats was not statistically significant ($p = 0.5$).

A similar analysis was conducted of the varicosities or fiber swellings that were present on these axon arbors (Fig. 2*D*). Numerous ultrastructural studies have shown these varicosities to be sites of synaptic contact (Ishizuka et al., 1990; Deitch et al., 1991; Gulyás et al., 1993; Sik et al., 1993). The number of varicosities within each concentric ring was counted. The results shown in Figure 9*B* are similar to those for axon intersections in Figure 9*A*. There seemed to be a tendency for fewer varicosities to be near the parent cell body. Nonetheless, these differences proved not to be statistically significant (repeated measures two-way ANOVA, $p = 0.66$) Likewise, when total axon length, number of axon branch points, varicosity number, and varicosity density per unit length of axon were analyzed, significant differences were not detected (Table 1).

DISCUSSION

When neurons from both hippocampus and neocortex are examined from patients with chronic focal epilepsy, they often show dramatic dendritic abnormalities (Ward, 1969; Isokawa and Levesque, 1991; Multani et al., 1994; Belichenko and Dahlstrom, 1995). Dendritic spine loss has been repeatedly reported and has been suggested to be more severe with an increasing duration of a seizure disorder (Multani et al., 1994). A decrease in dendritic branching is commonly observed. Moreover, the dendrites of pyramidal cells have also been reported to have varicose swellings at irregular intervals along their length. Similar observations have been made in a genetic model of epilepsy (Paul et al., 1981) and accompanying focal epilepsy induced by local injection of alumina or ferric chloride (Westrum et al., 1964; Reid et al., 1979; Willmore et al., 1980). Spine loss and varicose swellings have also been reported in explant cultures of hippocampus after prolonged (3 d) exposure to convulsant drugs (Müller et al., 1993)

One major difference in results presented here and in these earlier studies is that the dendrites from epileptic rats did not demonstrate varicose swellings. The reason for this has yet to be determined. However, it seems likely that dendritic varicose swellings are acute responses of pyramidal cells to ongoing seizure activity. In the tetanus toxin model used here, seizures occur in adulthood in 50% of animals, and their frequency can be low and duration short. Thus, the likelihood of observing acute responses to seizures, such as dendritic varicose swellings, might be low. In keeping with our findings are results from studies of CA_1 pyramidal cells in rats that were treated as adults with tetanus toxin. Varicose swellings on dendrites were not reported, although a small decrease in the complexity of dendritic branching was observed (Colling et al., 1996). Varicose swellings of dendrites have been reported immediately after seizures induced by convulsants (Evans et al., 1983) and sustained electrical stimulation of afferents to hippocampus (Sloviter, 1983). They have also been reported in response to application of excitatory amino acids and their analogs both *in vivo* (Olney et al., 1979; Sloviter and Dempser, 1985) and *in vitro* (Park et al., 1996). Other *in vitro* studies have reported dendritic swellings in response to hypoxia–ischemia and electrographic seizures induced by convulsants (Müller et al., 1993; Park et al., 1996) in which excessive glutamate is thought to be released. In terms of the tetanus toxin model, if varicose swellings are an acute response to seizures, such swellings would be more likely to be observed during the first week after toxin injection when seizure frequency is so high. However, these experiments have yet to be performed.

Another feature of neurons in rats treated with tetanus toxin in infancy is the dramatic decrease in the diameter of the dendritic shafts. (Figs. 4*D*, 5; Table 1) Similar alterations in dendritic

diameter have not been reported in previous studies. In some instances, this may simply have been overlooked. However, in other studies the morphological alterations of neurons may have been so severe and segmental loss so significant that decreases in dendritic diameter may have been hard to evaluate because comparisons to segments of the same branch order in control specimens would be difficult.

Potential mechanisms producing dendritic abnormalities

Dendrotoxicity

One mechanism that might contribute to dendritic changes in epilepsy is excitotoxicity. Hippocampal seizures are thought to be mediated in large part by excitatory synapses on dendrites that use glutamate as their neurotransmitter (Swann et al., 1986, 1993). This is certainly true in the CA_3 subfield in which recurrent excitatory collaterals are so extensive (Ishizuka et al., 1990; Li et al., 1994; Gomez-DiCesare et al., 1997) and especially in infancy when the hippocampus is so susceptible to seizures (Swann and Brady, 1984). However, the developing hippocampus is also noteworthy for its invulnerability to seizure-induced cell death (Nitecka et al., 1984; Okada et al., 1984; Cavalheiro et al., 1987).

In the tetanus toxin model, a visual inspection of hippocampus in adulthood was unable to detect neuronal cell loss (Lee et al., 1995). However, recent cell counts of neurons in stratum pyramidale detected a small (13%) but significant decrease in neuronal number that was restricted to the CA_{3C} subfield (C. L. Lee, unpublished observations). This finding may be consistent with results presented in this paper. For instance, segmental loss observed in basilar dendrites (Table 1) could be the result of a localized excitotoxic insult to basilar dendrites. Basilar dendrites receive the majority of recurrent excitatory synapses in area CA_3 (Gomez-DiCesare et al., 1997). Thus, it is possible that nonlethal excitotoxic damage to dendrites of CA_{3C} neurons may take place during recurrent seizures and may contribute to the dendritic abnormalities reported in this paper. Some cells may receive a severe excitotoxic insult and die.

Deafferentation and developmental plasticity

Numerous studies have shown that the elimination of afferent pathways to neurons can lead to a loss of dendritic spines (Hámori, 1973; Parnavelas et al., 1974; Matthews et al., 1976; Represa et al., 1991). Results from such studies led earlier investigators to propose that spine loss in neurons taken from humans and animals with epilepsy is caused by a partial deafferentation of pyramidal cells (Ward, 1969; Paul and Scheibel, 1986). In experiments reported here, CA_3 pyramidal cells did not demonstrate a loss of recurrent excitatory collaterals (Figs. 8, 9). Thus, the synapses that mediate seizures in local CA_3 circuits appear to be present. If the dendrites of CA_{3C} pyramidal cells are deafferented, then the missing synapses must arise from a source other than recurrent excitatory collaterals. In other words, deafferentation may be selective. During nervous system development, axon arbors and synapses anatomically remodel. This is also the case for local circuits in developing hippocampus (Gomez-DiCesare et al., 1997). The process of synapse selection is generally thought to be dependent on Na^+ action potential-based activity (Katz and Shatz, 1996) and is likely mediated by the NMDA receptor as a detector of coincident activity (Constantine-Paton et al., 1990). It is thought that correlated activity leads to a consolidation of coincidentally activated synapses (Constantine-Paton et al., 1990). Noncoincidentally active synapses are thought to undergo heterosynaptic long-term depression (LTD) (Singer, 1995). The repeated induction of LTD in these synapses has been proposed to lead to the pruning of unneeded axons. Recently, we wondered if synchronous network discharging, which leads to a persistence of epileptiform discharging in CA_3 network, might produce LTD of afferent pathways that were not participating in the generation of network bursts. Results from experiments demonstrated that epileptiform activity in the CA_3 network can produce LTD of inactive afferent pathways (Smith and Swann, 1996). Thus, the earlier suggestions (Ward, 1969) that epileptic neurons are partially deafferented may be correct. However, the deafferentation may be selective and mediated by processes that normally mediate synapse selection during network development.

Mechanisms of epileptogenesis

The physiological mechanisms that are responsible for epileptiform discharging in this chronic model of epilepsy remain to be determined. It is hard to envision how a selective deafferentation that might underlie spine loss could be responsible for epilepsy. A loss of excitatory input onto dendrites would be expected to decrease, not increase, excitability. On the other hand, spine loss and an associated deafferentation could contribute to other behavioral sequelae of epilepsy. For instance, children with a history of recurrent seizures have been reported to have low IQs (Bourgeois et al., 1983; Rodin et al., 1986; Holmes, 1991). Indeed, adult rats treated with tetanus toxin as infants have recently been shown to be impaired in their ability to acquire spatial memories (Lee et al., 1997).

The dramatic decrease in dendritic diameter reported here could result in alterations in synaptic integration and signal propagation within dendrites. In a previous study (Smith et al., 1998), recordings from CA_{3C} cells detected no significant differences in intrinsic properties of these neurons, although a small number of neurons had prolonged intrinsic bursts, which may be indicative of dendritic hyperexcitability. It is possible that the level of expression and distribution of Na^+, Ca^{+2}, and/or K^+ channels in dendritic membranes in epileptic rats may be abnormal. However, further studies will be required to explore these issues.

Alterations in channel density or distribution on dendritic segments would also be expected to significantly modify the effectiveness of synaptic transmission. Furthermore, alterations in the distribution of recurrent excitatory synapses on dendrites could lead to an enhanced ability of these synapses to produce action potentials and, in turn, promote the reverberation of recurrent excitation in networks of mutually excitatory pyramidal cells. We have previously shown that bath application of picrotoxin to slices from epileptic rats leads to prolonged electrographic seizure activity that is never observed in slices from saline-injected control rats (Smith et al., 1998). These results not only suggest that $GABA_A$ receptor-mediated synaptic inhibition is important in controlling seizures in epileptic rats, but that once eliminated, the full potential of recurrent excitatory networks to produce seizures is unleashed. Because this potential is far greater in epileptic rats, either an underlying alteration in intrinsic excitability, most likely arising from dendrites, and/or highly effective recurrent excitatory synapses contribute importantly to seizures in this chronic model of early-onset epilepsy.

REFERENCES

Anderson AE, Hrachovy RA, Swann JW (1997) Increased susceptibility to tetanus toxin-induced seizures in immature rats. Epilepsy Res 26:433–442.

Belichenko PV, Dahlstrom A (1995) Studies on the 3-dimensional architecture of dendritic spines and varicosities in human cortex by confocal laser scanning microscopy and lucifer yellow microinjections. J Neurosci Methods 57:55–61.

Bourgeois BFD, Prensky AL, Palkes HS, Talent BK, Busch SG (1983) Intelligence in epilepsy: a prospective study in children. Ann Neurol 14:438–444.

Buckmaster PS, Strowbridge BW, Schwarrtzkroin PA (1993) A comparison of rat hippocampal mossy cells and CA3c pyramidal cells. J Neurophysiol 70:1281–1299.

Catala I, Ferrer I, Galofre E, Fabregues I (1988) Decreased numbers of dendritic spines on cortical pyramidal neurons in dementia. A quantitative Golgi study on biopsy sample. Hum Neurobiol 6:255–259.

Cavalheiro EA, Silva DF, Turski WA, Calderazzo-Filho LS, Bortolotto ZA, Turski L (1987) The susceptibility of rats to pilocarpine-induced seizures is age-dependent. Dev Brain Res 37:43–58.

Chicurel ME, Harris KM (1992) Three-dimensional analysis of the structure and composition of CA3 branched dendritic spines and their synaptic relationships with mossy fiber boutons in the rat hippocampus. J Comp Neurol 325:169–182.

Claiborne BJ, Amaral DG, Cowan WM (1986) A light and electron microscopic analysis of the mossy fibers of the rat dentate gyrus. J Comp Neurol 246:435–458.

Collin C, Miyaguchi K, Segal M (1997) Dendritic spine density and LTP induction in cultured hippocampal slices. J Neurophysiol 17: 1614–1623.

Colling SB, Man WD-C, Draguhn A, Jefferys JGR (1996) Dendritic shrinkage and dye-coupling between rat hippocampal CA1 pyramidal cells in the tetanus toxin model of epilepsy. Brain Res 741:38–43.

Constantine-Paton M, Cline HT, Debski E (1990) Patterned activity, synaptic convergence, and the NMDA receptor in developing visual pathways. Annu Rev Neurosci 13:129–154.

Cross RG, Globus A (1978) Spine stems on tectal interneurons in jewel fish are shortened by social stimulation. Science 200:787–789.

Dailey ME, Smith SJ (1996) The dynamics of dendritic structure in developing hippocampal slices. J Neurosci 16:2983–2994.

Dalva MB, Ghosh A, Shatz CJ (1994) Independent control of dendritic and axonal form in the developing lateral geniculate nucleus. J Neurosci 14:3588–3602.

Deitch JS, Smith KL, Swann JW, Turner JN (1991) Ultrastructural investigation of neurons identified and localized using the confocal scanning laser microscope. J Electron Microsc 18:82–90.

Evans M, Griffiths T, Meldrum B (1983) Early changes in the rat hippocampus following seizures induced by bicuculline or L-allylglycine: a light and electron microscope study. Neuropathol Appl Neurobiol 9:39–52.

Falconer MA, Serafetinides EA, Corsellis JAN (1964) Etiology and pathogenesis of temporal lobe epilepsy. Arch Neurol 10:233–248.

Ferrer I, Roig C, Espino A, Peiro G, Matias-Guiu X (1991) Dementia of frontal lobe type and motor neuron disease: a Golgi study of the frontal cortex. J Neurol Neurosurg Psychiatry 54:932–934.

Gomez-DiCesare CM, Smith KL, Rice F, Swann J (1997) Axonal remodeling during postnatal maturation of CA_3 hippocampal pyramidal neurons. J Comp Neurol 384:165–180.

Gulyás AI, Miles R, Sík A, Tóth K, Tamamaki N, Freund TF (1993) Hippocampal pyramidal cells excite inhibitory neurons through a single release site. Nature 366:683–687.

Hámori J (1973) The inductive role of presynaptic axons in the development of postsynaptic spines. Brain Res 62:337–344.

Hoffman DA, Magee JC, Colbert CM, Johnston D (1997) K^+ channel regulation of signal propagation in dendrites of hippocampal pyramidal neurons. Nature 387:869–875.

Holmes GL (1991) The long-term effects of seizures on the developing brain: clinical and laboratory issues. Brain Dev 13:393–409.

Hosokawa T, Rusakov DA, Bliss TVP, Fine A (1995) Repeated confocal imaging of individual dendritic spines in the living hippocampal slice: evidence for changes in length and orientation associated with chemically induced LTP. J Neurosci 15:5560–5573.

Ishizuka N, Weber J, Amaral DG (1990) Organization of intrahippocampal projections originating from CA3 pyramidal cells in the rat. J Comp Neurol 295:580–623.

Isokawa M, Levesque MF (1991) Increased NMDA responses and dendritic degeneration in human epileptic hippocampal neurons in slices. Neurosci Lett 132:212–216.

Isokawa M, Levesque M, Fried I, Engel JJ (1997) Glutamate currents in morphologically identified human dentate granule cells in temporal lobe epilepsy. J Neurophysiol 77:3355–3369.

Johnston D, Magee JC, Colbert CM, Christie BR (1996) Active properties of neuronal dendrites. Annu Rev Neurosci 19:165–186.

Katz LC, Shatz CJ (1996) Synaptic activity and the construction of cortical circuits. Science 274:1133–1138.

Lee CL, Hrachovy RA, Smith KL, Frost Jr JD, Swann JW (1995) Tetanus toxin-induced seizures in infant rats and their effects on hippocampal excitability in adulthood. Brain Res 677:97–109.

Lee CL, Hannay HJ, Rashid S, Hrachovy R, Swann J (1997) Persistent deficits in acquisition of spatial memories following repeated seizures in early-life. Neurosci Abstr 23:1591.

Leuba G, Garey LJ (1984) Development of dendritic patterns in the lateral geniculate nucleus of monkey: a quantitative Golgi study. Dev Brain Res 16:285–299.

Li X-G, Somogyi P, Ylinen A, Buzsáki G (1994) The hippocampal CA3 network: an *in vivo* intracellular labeling study. J Comp Neurol 339:181–208.

Magee JC, Johnston D (1995) Characterization of single voltage-gated Na^+ and Ca^{2+} channels in apical dendrites of rat CA1 pyramidal neurons. J Physiol (Lond) 487:67–90.

Mantyh PW, DeMaster E, Malhotra A, Ghilardi JR, Rogers SD, Mantyh CR, Liu H, Basbaum A, Vigna SR, Maggio JE, Simone DA (1995) Receptor endocytosis and dendrite reshaping in spinal neurons after somatosensory stimulation. Science 268:1629–1632.

Matthews DA, Cotman C, Lynch G (1976) An electron microscopic study of lesion-induced synaptogenesis in the dentate gyrus of the adult rat. I. magnitude and time course of degeneration. Brain Res 115:1–21.

Moser M-B, Trommald M, Andersen P (1994) An increase in dendritic spine density on hippocampal CA1 pyramidal cells following spatial learning in adult rats suggests the formation of new synapses. Proc Natl Acad Sci USA 91:12673–12675.

Müller M, Gähwiler BH, Rietschin L, Thompson SM (1993) Reversible loss of dendritic spines and altered excitability after chronic epilepsy in hippocampal slice cultures. Proc Natl Acad Sci USA 90:257–261.

Multani P, Myers RH, Blume HW, Schomer DL, Sotrel A (1994) Neocortical dendritic pathology in human partial epilepsy: a quantitative Golgi study. Epilepsia 35:728–736.

Nitecka L, Tremblay E, Charton G, Bouillot JP, Berger ML, Ben-Ari Y (1984) Maturation of kainic acid seizure-brain damage syndrome in the rat. II. Histopathological sequelae. Neuroscience 13:1072–1094.

Okada R, Moshe SL, Albala BJ (1984) Infantile status epilepticus and future seizures susceptibility in the rat. Dev Brain Res 15:177–183.

Olney JW, Fuller T, de Gubareff T (1979) Acute dendrotoxic changes in the hippocampus of kainate treated rats. Brain Res 176:91–100.

Park JS, Bateman MC, Goldberg MP (1996) Rapid alterations in dendrite morphology during sublethal hypoxia or glutamate receptor activation. Neurobiol Dis 3:215–227.

Parnavelas JG, Lynch G, Brecha N, Cotman CW, Globus A (1974) Spine loss and regrowth in hippocampus following deafferentation. Nature 248:71–73.

Paul LA, Fried I, Watanabe K, Forsythe AB, Scheibel AB (1981) Structural correlates of seizure behavior in the mongolian gerbil. Science 213:924–926.

Paul LA, Scheibel AB (1986) Structural substrates of epilepsy. In: Advances in Neurology (Delgado-Escueta AV, Ward Jr AA, Porter RJ, eds), pp 775–786. New York: Raven.

Purpura DP, Bodick N, Suzuki K, Rapin I, Wurzelmann S (1982) Microtubule disarray in cortical dendrites and neurobehavioral failure. 1. Golgi and electron microscopic studies. Brain Res 281:287–297.

Reid SA, Sypert GW, Boggs WM, Willmore LJ (1979) Histopathology of the ferric-induced chronic epileptic focus in cat: a Golgi study. Exp Neurol 66:205–219.

Represa A, Dessi F, Beaudoin M, Ben-Ari Y (1991) Effects of neonatal gamma-ray irradiation on rat hippocampus-I. postnatal maturation of hippocampal cells. Neuroscience 42:137–150.

Rhin LL, Claiborne BJ (1990) Dendritic growth and regression in rat dentate granule cells during late postnatal development. Dev Brain Res 54:115–124.

Rodin EA, Schmaltz S, Twitty G (1986) Intellectual functions of patients with childhood-onset epilepsy. Dev Med Child Neurol 28:25–33.
Sholl DA (1955) The organization of the visual cortex in cat. J Anat (Lond) 89:33–46.
Sik A, Tamamaki N, Freund TF (1993) Complete axon arborization of a single CA3 pyramidal cell in the rat hippocampus, and its relationship with postsynaptic parvalbumin-containing interneurons. Eur J Neurosci 5:1719–1728.
Singer W (1995) Development and plasticity of cortical processing architectures. Science 270:758–764.
Sloviter RS (1983) "Epileptic" brain damage in rats induced by sustained electrical stimulation of the perforant path. I. Acute electrophysiological and light microscopic studies. Brain Res Bull 10:675–697.
Sloviter RS, Dempser DW (1985) "Epileptic" brain damage is replicated qualitatively in the rat hippocampus by central injection of glutamate or aspartate but not by GABA or acetylcholine. Brain Res Bull 15:39–60.
Smith KL, Swann JW (1996) Long term depression of perforant path epsps following synchronous network bursting in immature hippocampus. Epilepsia 37:73.
Smith KL, Szarowski DH, Turner JN, Swann JW (1995) Diverse neuronal populations mediate local circuit excitation in area CA_3 of developing hippocampus. J Neurophysiol 74:650–672.
Smith KL, Lee CL, Swann JS (1998) Local circuit abnormalities inchronically epileptic rats after intrahippocampal tetanus toxin injection in infancy. J Neurophysiol 79:106–116.
Spruston N, Schiller Y, Stuart G, Sakmann B (1995) Activity-dependent action potential invasion and calcium influx into hippocampal CA1 dendrites. Science 268:297–300.
Swann J, Jiang MH, Smith K, Lee C (1996) Early-life seizures: can synaptic plasticity produce neuropathology? Neurosci Abstr 26:2098.
Swann JW, Brady RJ (1984) Penicillin-induced epileptogenesis in immature rat CA3 hippocampal pyramidal cells. Dev Brain Res 12:243–254.
Swann JW, Brady RJ, Friedman RJ, Smith EJ (1986) The dendritic origins of penicillin-induced epileptogenesis in CA3 hippocampal pyramidal cells. J Neurophysiol 56:1718–1738.
Swann JW, Smith KL, Brady RJ (1993) Localized excitatory synaptic interactions mediate the sustained depolarization of electrographic seizures in developing hippocampus. J Neurosci 13:4680–4689.
Ward AAJ (1969) The epileptic neuron: chronic foci in animals and man. In: Basic mechanisms of the epilepsies (Jasper HH, Ward AA, Pope A eds), pp 263–298. Boston: Little, Brown.
Westrum LE, White LEJ, Ward AAJ (1964) Morphology of the experimental epileptic focus. J Neurosurg 21:1033–1046.
Willmore LJ, Ballinger WEJ, Boggs W, Sypert GW, Rubin JJ (1980) Dendritic alterations in rat isocortex within an iron-induced chronic epileptic focus. Neurosurgery 7:142–146.
Woolley CS, Gould E, Frankfurt M, McEwen BS (1990) Naturally occurring fluctuations in dendritic spine density on adult hippocampal pyramidal neurons. J Neurosci 10:4038–4039.